



## Utilizing Remote Sensing Data to Evaluate the Urban Heat Island: A Case Study of Quetta City, Balochistan

Zakaria Shah<sup>1</sup>, Romana Ambreen<sup>2</sup>, Niamat Ullah<sup>3</sup>, Shafi Ullah<sup>4</sup> & Syed Wajid Hanif Bukhari<sup>5</sup>

<sup>1</sup>M.Phil Scholar, Department of Geography and Regional Planning, University of Balochistan, Quetta 87300, Pakistan, Email: [zakariashah3@gmail.com](mailto:zakariashah3@gmail.com)

<sup>2</sup>Associate Professor, Department of Geography and Regional Planning, University of Balochistan, Quetta 87300, Pakistan, Email: [ambgeog@gmail.com](mailto:ambgeog@gmail.com)

<sup>3</sup>Research Assistant, Spatial Decision Support System (SDSS) Lab, National Center of GIS and Space Applications (NCGSA), Balochistan University of Information Technology, Engineering and Management Sciences (BUITEMS), Quetta 87300, Pakistan, Email: [niamatullahza@gmail.com](mailto:niamatullahza@gmail.com)

<sup>4</sup>Assistant Professor, Department of Computer Engineering, Balochistan University of Information Technology, Engineering and Management Sciences (BUITEMS), Quetta 87300, Pakistan, Email: [shafi.ullah@buitms.edu.pk](mailto:shafi.ullah@buitms.edu.pk)

<sup>5</sup>Assistant Professor, Centre of Excellence in Mineralogy, University of Balochistan, Quetta 87300, Pakistan, Email: [wajid.cem@um.uob.edu.pk](mailto:wajid.cem@um.uob.edu.pk)

### ARTICLE INFO

#### Article History:

Received: February 17, 2025  
Revised: March 15, 2025  
Accepted: March 18, 2025  
Available Online: March 19, 2025

#### Keywords:

Urban heat island (UHI), MODIS, Land Surface Temperature (LST), Quetta, Balochistan

#### Corresponding Author:

Niamat Ullah

#### Email:

[niamatullahza@gmail.com](mailto:niamatullahza@gmail.com)

### ABSTRACT

The urban heat island (UHI) effect presents a significant environmental challenge in rapid urbanization. Its mitigating impacts on public health, power consumption, and urban livability require a brief understanding of energy dynamics. MODIS satellite data, has detailed spatial and temporal coverage that serves as an essential tool in analyzing temperature trends, changes in land cover, and other related variables. Therefore, this study leverages MODIS data to analyze the impact of UHI, identifying significant changes in temperature distribution patterns over time. Our results inferred expansion in the high-temperature zone, shrinking in the central temperature zone, and comparatively stable in the low-temperature zone. These trends align with the trajectory of global warming and emphasize a wide-ranged impact on the ecosystem, weather patterns, and human activities. These findings trend a pronounced peak in global warming during the months observed for rainfall, underscoring a clear connection to climate change. However, the analysis highlights the limitations of short-term datasets in capturing long-term UHI trends and calls for more comprehensive temporal data to visualize geographic complexity. urbanization and climate change in the region It provide the basis for creating sustainable urban planning strategies and important step towards achieving climate-friendly urban ecosystems that can mitigate the cascading effects of global warming.



## **Introduction**

Howard, 1810 describes the warmer temperatures in urban areas compared to surrounding rural areas, considering the urban heat island (UHI) effect. This variant temperature includes human activities with urbanization processes, the interaction between changing surface energy, dynamics of human heat release, and pollution in the atmosphere (Agan Ocukka et al., 2021). The UHI, therefore, is widely recognized as one of the leading examples of anthropogenic climate change (Liu, Peng, et al., 2017) and presents enormous challenges for the urban environment and its long-term sustainability. Urbanization resulting from the replacement of natural vegetation with impervious surfaces such as concrete, asphalt, etc., is the main driver of the urban heat island effect (UHI) (Ahmed, Kamruzzaman et al., 2013). This change disturbs the natural energy balance and resulting in the temperature inside the city's core increases. Research shows that changes in land use Especially the changing environment in developed cities. since the forest Agricultural fields and open space play an important role in intensifying the urban heat island effect (UHI) (Li et al., 2019). The biggest contributor to UHI is the shift in land usage from natural to impermeable surface (Li, Zhou et al. 2019). Agricultural, residential, and transitional/barren land cover types irradiance and the amount of vegetation present, all have strong negative correlations with each other. This implies that irradiance is significantly influenced by the amount of vegetation. Urban heat islands were more likely to form near the city center because of the preponderance of forests, agricultural uses, and residential uses connected to varying amounts of tree cover (Lo, Quattrochi et al. 1997).

Human-oriented urbanization and related land use by changing the natural landscape into an impervious surface have a substantial impact on the thermal climate of cities and their surrounding areas (Qiao, Liu et al. 2020). Comparative to the total population of a city, UHI is more closely related to neighborhood-level population density (Steenefeld, Koopmans et al. 2011). Factors such as the relative population density, degree of urbanization, and geographic characteristics of nearby communities for UHI severity and extent are closely affected that can be discovered by examining the fluctuations in temperature differences between urban, suburban, and rural stations (Zhang, Wang, et al. 2010). Therefore, human activities such as construction for the emergence of UHI are the clearest signs of urban climate change (Qiao, Liu, et al. 2010) where it causes discomfort for prolonged heat illness and death in high-temperature zones (Nuruzzaman, 2015, Lee, Din, et al., 2017). Due to high population densities and inadequate urban planning, especially during summer, there is an urgent need for sustainable urban development. Moreover, it will also increase the demand for cooling energy, and greenhouse gas emissions and worsen air quality, thus amplifying the environmental impact.

The UHI variability was temporal and spatially well documented with its intensity typically peaking during the hours shortly after sunset. Their urban surface geometry, building materials, anthropogenic heat sources, and pollution levels influence UHI. Therefore, due to the intricate thermal characteristics of urban environments, accurately simulating these complex interactions remains a significant challenge (Bottyan and Unger, 2003). However, urban planning interventions, such as incorporating green spaces and optimizing infrastructure design, play a pivotal role in moderating UHI intensity. Based on future projections, its effect will become an urgent challenge as urbanization intensifies. United Nations reports that 60% of the global population is expected to live in urban areas by 2030, further amplifying the need for effective mitigation strategies and policies to address the growing pressures associated with UHI. Its implications on energy usage, water ecosystems, tropospheric ozone, and overall livability (Chun and Guldmann, 2014) indicate the need for an approach at the urban planning and designing level.

Mitigating measures such as sustainable urban design, increased vegetation cover, and the implementation of energy-efficient infrastructure should be prioritized to minimize the adverse impacts of UHI. Understanding the dynamics of UHI interacting with urbanization, climate change, and surface energy exchange is important for designing targeted interventions. The research study aims to explore the drivers of UHI and its consequences, as well as provide insights into effective strategies for reducing UHI impacts in urban environments. and their residents.

## Data and Methods

### Study area

Quetta is Balochistan, Pakistan's capital and most populous city (Ullah, et al., 2024). Quetta is at a geographical location of longitude 66.9750° E and latitude 30.1798° N, at an elevation of 1,680 meters or 5,510 feet above the mean sea level (MSL) and covers an area of about 3,501 km<sup>2</sup> in total. It has a cold semi-arid climate and falls into the Köppen BSk category, with highly seasonal temperature variations. Summers, from late May to early September, average between 24°C and 26°C or 75-79°F, and the highest ever recorded was 42°C or 108°F on July 10, 1998. Autumn months start from mid-September and end at mid-November, with an average ranging from 12°C to 18°C or 54-64°F. Winters, late November to late February, are very cold with average temperatures ranging from 4°C to 5°C (39-41°F); the lowest recorded temperature was -18.3°C (0.9°F) on January 8, 1970. Spring starts early March and lasts till mid-May, with moderate average temperatures around 15°C (59°F).

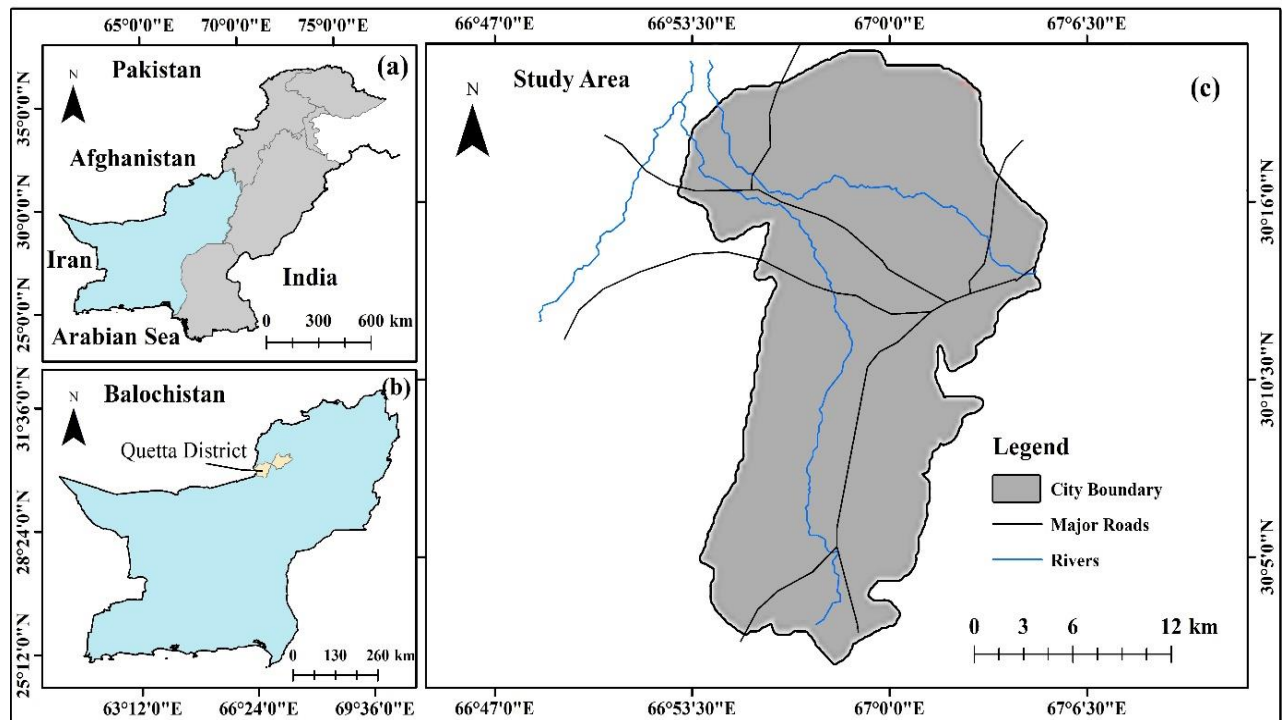


**Figure 1.** (a) Pakistan, (b) Balochistan, and (c) map of Quetta City, respectively.

### Methodology Data Analysis

The UHI of Quetta city was derived using two MODIS products, MOD11\_L2 and MYD11\_L2, which provide instantaneous views of the (Land Surface Temperature) LST at a 1-km resolution,

twice daily (two at night and two at day time photos), respectively. Since the availability of the satellite-derived LST is determined by objective factors (such as cloudiness), we have chosen three images from each month between January 1990 and 2020 that have at least one pixel with LST registered in the administrative perimeter of Quetta. These images are from the day and nighttime bands of the images. The nighttime LST is retrieved between 19.10 and 01.20 UTC, and the daytime pictures span the hours of 08.15 to 12.15 UTC.

Data from the CRU Climate Research Unit was collected for the years 1992, 2000, 2010, and 2020 for October and November to do additional analysis. We further extracted spatial and temporal data using USGS to analyze Urban Heat Islands (UHIs) using MOD11\_L2 (MODIS Terra Land Surface Temperature) and MYD11\_L2 (MODIS Aqua Land Surface Temperature).

The extracted data in HDF were further converted to GeoTIFF using GIS software and clipped for the area of interest to reduce processing time. To ensure more accurate temperature readings, the quality assessment (QA) layer filters out cloudy pixels and extracts the LST data from both (MOD11\_L2 and MYD11\_L2) models.

Using the following formula:

$$LST = \frac{K_2}{\ln\left(\frac{K_1}{L_\lambda} + 1\right)}$$

Where  $K_1$  and  $K_2$  are the band-specific thermal constants for MODIS,  $L_\lambda$  the spectral radiance derived from MODIS thermal bands, and  $\ln$  represents the natural logarithm.

### **Urban Heat Island (UHI) Calculation**

- We computed the variation between LST in urban and rural areas to identify UHI effects using:

$$UHI = LST_{\text{urban}} - LST_{\text{rural}}$$

UHI represents the urban heat island intensity,  $LST_{\text{urban}}$  is the Land Surface Temperature (LST) of the urban area, and  $LST_{\text{rural}}$  is the LST of the rural area.

- Tools like zonal statistics were used to extract precise temperature data across changed land use types.
- Temperature gradient maps were generated across urban and rural regions using GIS software (ArcGIS) to visualize LST variations.
- UHI intensities were visualized using heat maps with interpolation techniques (IDW, Kriging) for smoother surfaces.
- Finally, to identify areas of UHI significant effects were extracted using these resulting maps and further analyzed.

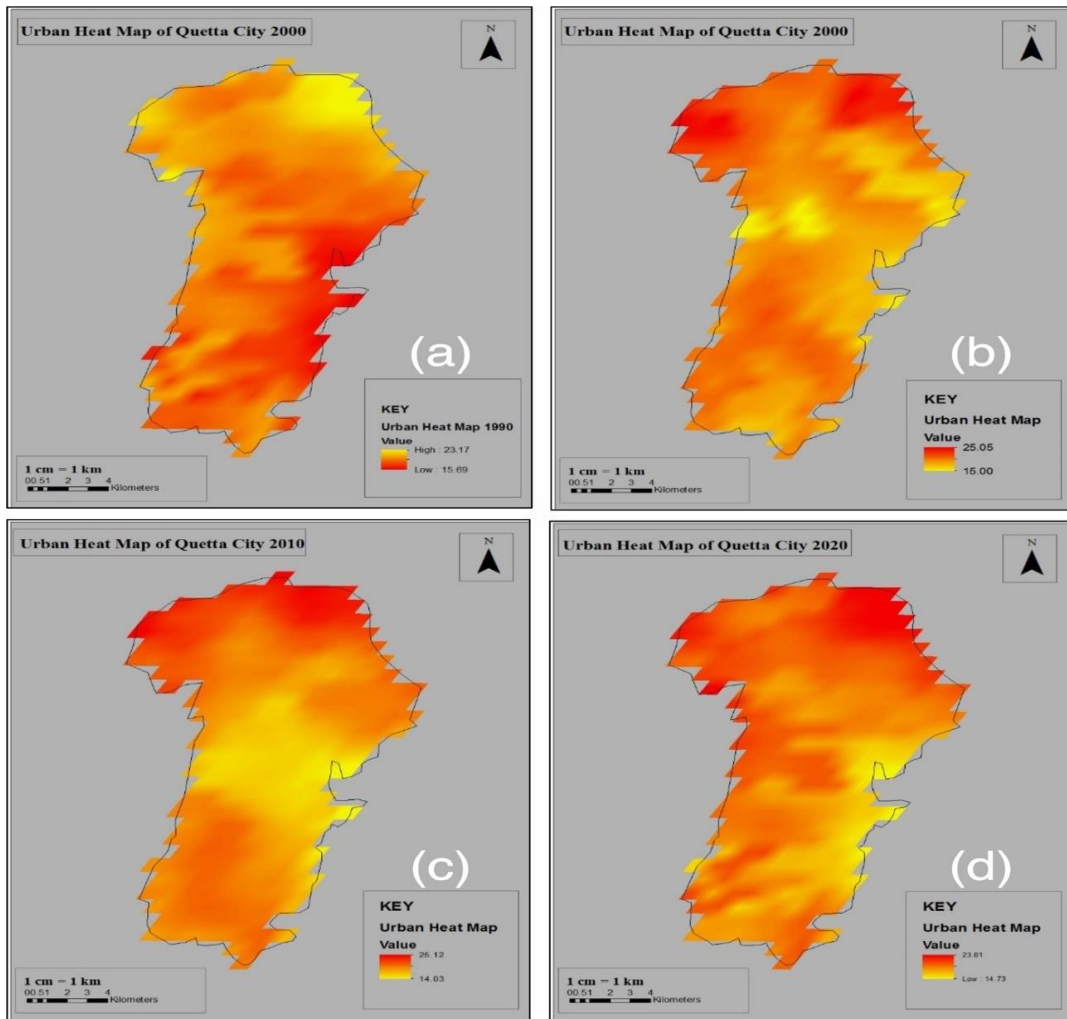


Figure 1. Urban Heat Maps for 1992 (a), 2000 (b), 2010 (c) and 2020 (d).

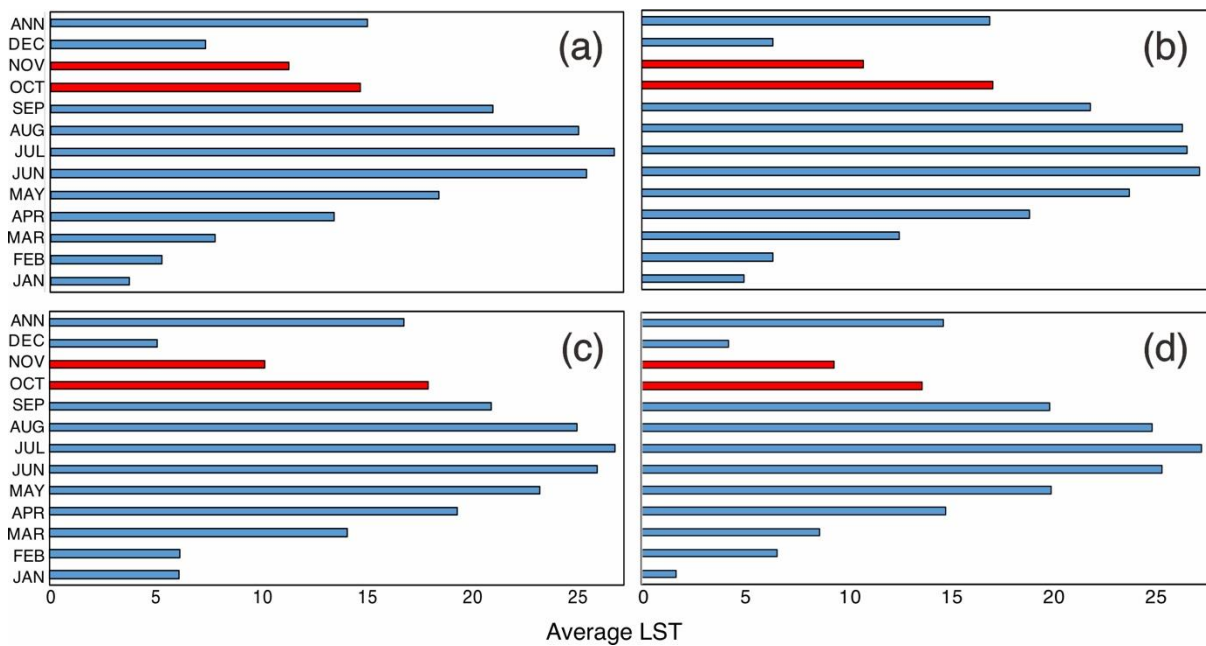
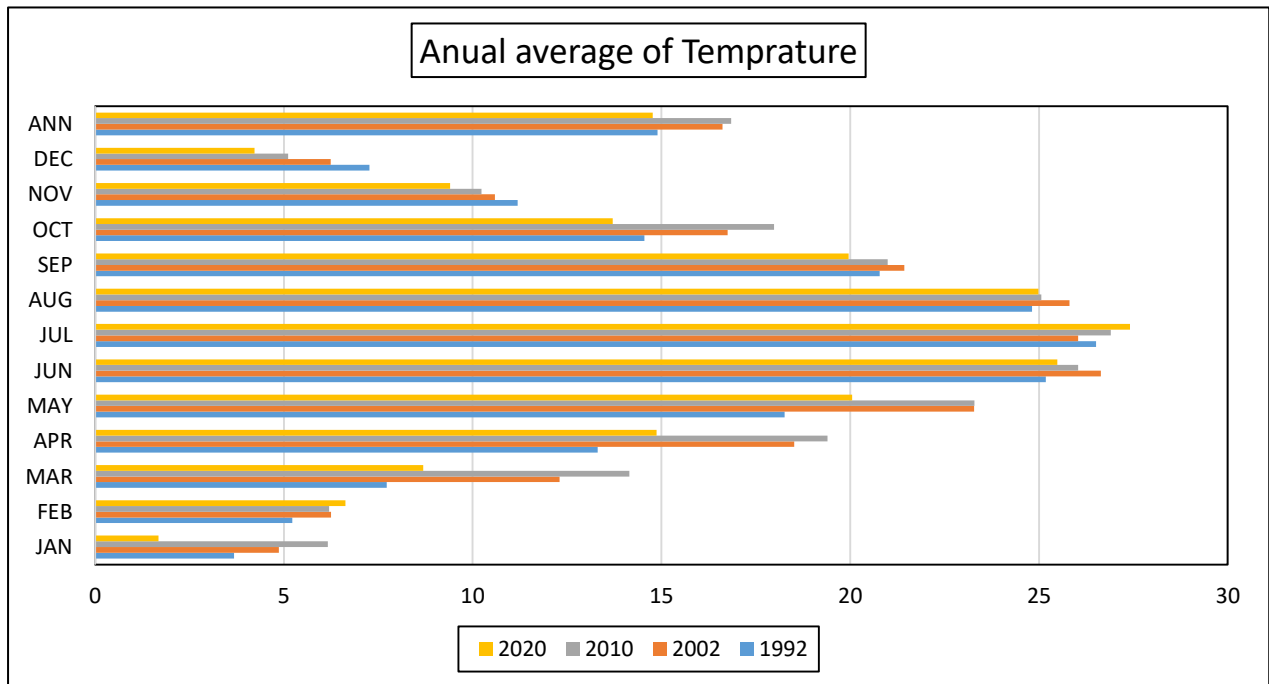


Figure 3. Average LST for each month across 1992 (a), 2000 (b), 2010 (c), and 2020 (d).

**Table 1: Maximum Temperatures of Years 1992,2002,2010,2020**

YEAR	JAN	FEB	MAR	APR	MAY	JUN	JUL	AUG	SEP	OCT	NOV	DEC	ANN
1992	3.68	5.22	7.72	13.31	18.26	25.18	26.51	24.82	20.78	14.55	11.19	7.27	14.9
2002	4.87	6.25	12.3	18.52	23.28	26.64	26.04	25.81	21.43	16.75	10.59	6.24	16.62
2010	6.16	6.2	14.15	19.4	23.29	26.04	26.9	25.06	20.99	17.98	10.23	5.11	16.85
2020	1.68	6.63	8.69	14.87	20.05	25.49	27.41	24.99	19.96	13.71	9.4	4.22	14.77



**Figure 4:** Annual Averages of Temperature for years 1992, 2000, 2010, and 2020.

### Results and Discussion

The data we used in our analysis contains average temperatures (°C; last column; ANN) for 1992, 2002, 2010, and 2020. Analysis reveals a clear and consistent upward trend that indicates continued warming in the region between 1992 and 2020. Among the years observed, 2010 was the warmest, with an average annual temperature of 16.85°C, and 1992 was the coolest, at 14.9°C. Across all years under examination, a discernible seasonal pattern is evident. The warmest temperatures occur during June, July, and August, corresponding to the summer season, whereas the coldest months are from December through February, representing winter. Of particular note is that July consistently emerges as the warmest month across all studied years. This seasonal trend emphasizes the expected temperature variability associated with climatic patterns and their seasonal progression.

The monthly temperature ranges exhibit notable variations over the analyzed years. During 1992, monthly temperatures fluctuated between a minimal 3.68°C in January and a maximum of 26.51°C in July. Similarly, in 2002, the temperature rose from 4.87°C in January to 26.64°C in June. During 2010, the temperature spectrum consistently increased from 5.11°C in December to 26.9°C in July, whereas in 2020, it decreased to 1.68°C in January and raised to 27.41°C in July. These variations

underscore interannual and intrapersonal changes, with July consistently increasing monthly average temperatures across all years.

Our data indicate a noticeable warming trend during May through September of the year overall study years. This suggests a potential shift toward progressively warmer transitional seasons, reflecting global climate trends. Furthermore, annual temperature variability is more pronounced during the cooler months (winter) compared to the summer period. Analysis of the years 2002, 2010, and 2020 reveals higher temperature fluctuations relative to 1992, suggesting increased interannual variability in recent decades.

The observed warming trends align with broader global warming patterns. Such increases in average temperature have far-reaching ecological, meteorological, and hydrological consequences, potentially impacting local weather patterns, ecosystems, agricultural productivity, and sea-level rise.

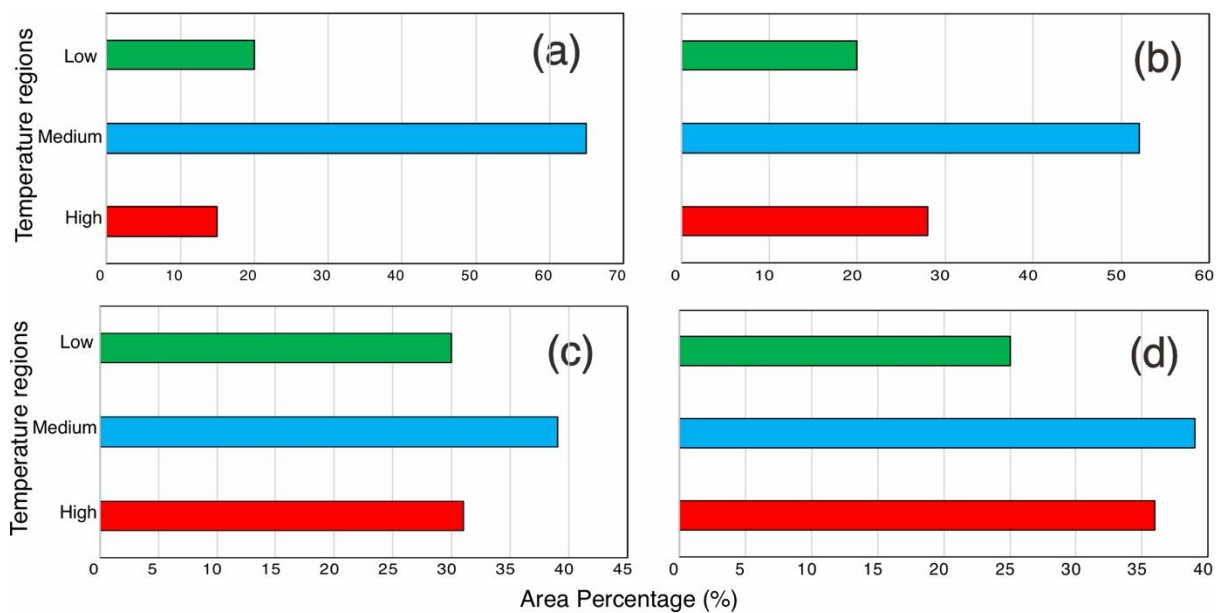


**Figure 5:** Temperatures regions with Areas Percentages for 1992 (a), 2000 (b), 2010 (c), and 2020 (d).

### Analysis of Temperature

The observed patterns also suggest significant spatial trends in temperature extremes. During 1992, 15% of observed areas recorded maximum temperature ranges. This proportion increased to 36% by 2020. It indicates a significant rise in regions experiencing higher maximum temperatures over time, likely attributed to global climate change, urbanization, and shifts in local environmental conditions. 65% of regions in 1992, exhibited mid-temperature ranges and declined to 39% in 2020. This reduction suggests a discernible shift toward more extreme temperature profiles, with a corresponding reduction in mid-temperature regions. This shift may stem from the expansion of both maximum and low-temperature extremes at the expense of mid-range temperatures.

In 1992, 20% of areas had low temperatures, experiencing a slight increase, stabilizing at 25% by 2020. While there is a slight upward trend, the changes in low-temperature areas are far less pronounced compared to those observed in the maximum and mid-temperature ranges. These

findings highlight the transformation in temperature distributions over the study period, with a clear shift toward extremes (both in maximum and minimum temperature categories) driven by climate change and regional environmental transformations. There are no observed trends of decreasing maximum temperatures in the analyzed areas. Instead, the percentage of maximum temperature areas has consistently increased from 1992 to 2020. Whereas mid-temperature areas from 1992 to 2020 have consistently decreased, suggesting a significant shift away. This decline points toward a potential redistribution of temperature zones, with regions transitioning into more extreme temperature ranges. Similarly, there is less clear decrease in low-temperature zones as observed for the maximum temperature regions, and remained relatively stable over the analyzed years.

Based on a relationship between LST variations and land use/land cover (LULC) changes, (Sadiq Khan, Ullah, et al., 2020) further highlights the growing UHI effect. This temperature rise has broad implications, impacting ecosystems, climate patterns, and sea levels. Analysis indicates a noticeable shift in temperature distribution over the years. The analyzed data provides strong evidence of an overall warming trend across the analyzed years, with the most pronounced warming observed during summer months and increasing interannual temperature variability. It also shows changes in temperature distribution with a noticeable increase in the extreme temperature and a shift away from the mid-level temperature profile. Therefore, these trends are consistent with global climate change models and emphasize the urgent need for targeted mitigation and adaptation strategies to manage environmental and social impacts.

## **Conclusion**

This analysis found impervious surfaces have increased significantly by 11.9%, using temporal Landsat data over the past 25 years, whereas other land-use categories have declined. Its cumulative impact of LULC changes on the city of Islamabad (between 1993 and 2018) represented an average warming effect of 1.52 °C. These findings align with the global trend of rising average temperatures over time, with an average cooling effect of 0.8 °C that affects ecosystem climate patterns and sea level. The main concluding remarks include; expansion in maximum temperature areas, decline in mid-temperature areas, and consistency or minor variations in low-temperature regions. Although our analysis shows strong evidence of climate change's influence on shifting temperature regimes, it still requires additional research, comprehensive datasets, and multidisciplinary analysis to understand the underlying causes of these shifts. Also, our analysis is merely based on a limited yearly and temporal dataset, therefore, expanding the analysis with longer periods and additional contextual factors would provide a broader and more nuanced understanding of these temperature trends. These models can drive a complex interplay of factors, including geographic location, urbanization, and regional climate dynamics. The increase in temperature and UHI is most important to understand. It may affect daily livability and climate as well. The calculations and analyzed data indicate the future alarming conditions. If this trend of increasing temperature and decreasing greenery continues, this may have many consequences on daily life, climate, agriculture, and wildlife as well.

**Acknowledgments:** The authors are grateful to the Spatial Data Support System (SDSS) Lab, NCGSA, BUIITEMS, for providing guidance and expert support for the present study.

**Author Contribution:** Zakaria Shah<sup>1</sup>, Romana Ambreen, Niamat Ullah; wrote, designed, analyzed, and interpreted the data; Shafi Ullah and Syed Wajid Hanif Bukhari; contributed materials, analysis tools, or data; wrote the paper.

**Funding:** The current research has not received any funding.

## References

1. Agan, P., Oukka, M., & Oku, P. (2021). Urban Heat Island Effects; A De-Greening Process, Implication for Environmental Sustainability and Quality of Urban Life. A Review.
2. Ahmed, B., Kamruzzaman, M., Zhu, X., Rahman, M. S., & Choi, K. (2013). Simulating Land Cover Changes and Their Impacts on Land Surface Temperature in Dhaka, Bangladesh. *Remote Sensing*, 5(11), 5969-5998.
3. Botlyán, Z., & Unger, J. (2003). A multiple linear statistical model for estimating the mean maximum urban heat island. *Theoretical and Applied Climatology*, 75, 233-243. doi: 10.1007/s00704-003-0735-7
4. Chun, B., & Guldmann, J. M. (2014). Spatial statistical analysis and simulation of the urban heat island in high-density central cities. *Landscape and Urban Planning*, 125, 76-88. doi: <https://doi.org/10.1016/j.landurbplan.2014.01.016>
5. Department, P. M. (2012). " Climate Data Processing Centre. Archived from the original on 13 June 2010. Retrieved 7 December 2019."
6. Karimi Firozjaei, M., Sedighi, A., Kiavarz, M., & Alavi Panah, S. K. (2018). Statistical analysis of surface urban heat island intensity variations: A case study of Babol city, Iran. *GIScience & Remote Sensing*, 56, 1-29. doi: 10.1080/15481603.2018.1548080
7. Lee, Y. Y., Din, M. F. M., Ponraj, M., Noor, Z. Z., Iwao, K., & Chelliapan, S. (2017). Overview of Urban Heat Island (UHI) phenomenon towards human thermal comfort. *Environmental Engineering and Management Journal*, 16, 2097-2111.
8. Li, H., Zhou, Y., Wang, X., Zhou, X., Zhang, H., & Sodoudi, S. (2019). Quantifying urban heat island intensity and its physical mechanism using WRF/UCM. *Science of the total environment*, 650, 3110-3119. doi: <https://doi.org/10.1016/j.scitotenv.2018.10.025>
9. Liu, Y., Peng, J., & Wang, Y. (2017). Diversification of Land Surface Temperature Change under Urban Landscape Renewal: A Case Study in the Main City of Shenzhen, China. *Remote Sensing*, 9(9), 919.
10. Lo, C. P., Quattrochi, D. A., & Luvall, J. C. (1997). Application of high-resolution thermal infrared remote sensing and GIS to assess the urban heat island effect. *International Journal of Remote Sensing*, 18(2), 287-304. doi: 10.1080/014311697219079
11. Nuruzzaman, M. (2015). Urban Heat Island: Causes, Effects and Mitigation Measures -A Review. *International Journal of Environmental Monitoring and Analysis*, 3, 67-73. doi: 10.11648/j.ijema.20150302.15
12. Qiao, Z., Liu, L., Qin, Y., Xu, X., Wang, B., & Liu, Z. (2020). The Impact of Urban Renewal on Land Surface Temperature Changes: A Case Study in the Main City of Guangzhou, China. *Remote Sensing*, 12(5), 794.
13. Steeneveld, G. J., Koopmans, S., Heusinkveld, B. G., van Hove, L. W. A., & Holtslag, A. A. M. (2011). Quantifying urban heat island effects and human comfort for cities of

- variable size and urban morphology in the Netherlands. *Journal of Geophysical Research: Atmospheres*, 116(D20). doi: <https://doi.org/10.1029/2011JD015988>
14. Stewart, I. D. (2011). A systematic review and scientific critique of methodology in modern urban heat island literature. *International Journal of Climatology*, 31(2), 200-217. doi: <https://doi.org/10.1002/joc.2141>
  15. Sadiq Khan, M., Ullah, S., Sun, T., Rehman, A. U., & Chen, L. (2020). Land-use/land-cover changes and its contribution to urban heat Island: A case study of Islamabad, Pakistan. *Sustainability*, 12(9), 3861.
  16. Ullah, N., Tariq, A., Qasim, S. et al. Geospatial analysis and AHP for flood risk mapping in Quetta, Pakistan: a tool for disaster management and mitigation. *Appl Water Sci* 14, 236 (2024). <https://doi.org/10.1007/s13201-024-02293-1>
  17. Wang, Y., Berardi, U., & Akbari, H. (2016). Comparing the effects of urban heat island mitigation strategies for Toronto, Canada. *Energy and Buildings*, 114, 2-19. doi: <https://doi.org/10.1016/j.enbuild.2015.06.046>
  18. Zhang, K., Wang, R., Shen, C., & Da, L. (2010). Temporal and spatial characteristics of the urban heat island during rapid urbanization in Shanghai, China. *Environ Monit Assess*, 169(1-4), 101-112. doi: 10.1007/s10661-009-1154-8.